Transport mechanisms in ZnO/CdS/$CuInSe_2$ solar cells

Ji-Beom Yoo,[a] Alan L. Fahrenbruch, and R. H. Bube
Department of Materials Science and Engineering, Stanford University, Stanford, California 94305

(Received 29 January 1990; accepted for publication 29 June 1990)

The transport mechanisms in ZnO/CdS/$CuInSe_2$ solar cells prepared by ARCO (now Siemens) Solar Inc. have been analyzed by measurements of current versus voltage at different temperatures in the dark, short-circuit current versus open-circuit voltage at different temperatures in the light, spectral response of quantum efficiency, and junction capacitance. In the dark, recombination in the depletion region and/or thermally assisted tunneling are the dominant transport mechanisms. The observation of a smaller open-circuit voltage than would be predicted from the dark transport parameters is the result of a small change in the transport parameters under illumination, probably without a change in transport mechanism.

I. INTRODUCTION

The use of thin-film semiconductors deposited on a low-cost substrate has been regarded as a promising approach toward the mass production of low-cost photovoltaic arrays for terrestrial power generation. Copper indium diselenide, $CuInSe_2$, has shown considerable promise as a candidate for thin-film solar cells. To date CdS has received the most attention as the best heterojunction partner for $CuInSe_2$ because CdS can be easily deposited by vacuum evaporation, and has a good lattice match with $CuInSe_2$ and a favorable electron affinity.[1,2] CdS/$CuInSe_2$ solar cells have demonstrated high efficiency, approaching 11% and good stability.[3] But in simple thin-film CdS/$CuInSe_2$ cells, there is a significant absorption loss in the front CdS layer, corresponding to a loss of about 7–8 mA/cm^2 in short-circuit current under AM 1.5 illumination.[4] Large band gap materials like ZnO, In_2O_3, ZnCdS, and SnO_2 can be viable alternatives for the window layer. ZnO has been used as a window layer by ARCO Solar (now Siemens Solar) Inc., showing 25% greater photocurrent than for a comparable device using a simple CdS window layer.[5] The ARCO cells do use a thin CdS film (< 500 Å) deposited between the ZnO and the $CuInSe_2$ to improve the junction properties.

Although characterization of the transport properties of CdS/$CuInSe_2$ cells has been extensively carried out,[6-14] similar characterization of the ZnO/CdS/$CuInSe_2$ cell has not yet been fully made. Understanding the transport properties of the cell is clearly an important ingredient in developing higher efficiency devices.

We have analyzed the transport properties of ZnO/CdS/$CuInSe_2$ solar cells fabricated by ARCO Solar Inc., using measurements of current versus voltage from 210 to 360 K in the dark, short-circuit current J_{SC} versus open-circuit voltage V_{OC} over this same temperature range, as well as spectral response of the cell, and dependence of the cell capacitance on frequency and applied voltage.

II. EXPERIMENTAL PROCEDURE

Figure 1 shows a schematic diagram of the ARCO ZnO/CdS/$CuInSe_2$/Mo/glass thin-film solar cell. A $CuInSe_2$ layer about 2 μm thick is deposited on Mo on glass, which acts as a back ohmic contact to the $CuInSe_2$. A thin (< 500Å) CdS layer is deposited as an intermediate layer to improve the interface properties and as a chemical buffer layer to protect the $CuInSe_2$ layer during subsequent processings. A ZnO layer deposited on the CdS acts as both a window layer and a partial antireflection coating. Mitchell has reported that ZnO texturing significantly reduces optical reflection to about 6%.[14]

Current versus voltage measurements were made with a Keithley 619 electrometer/multimeter and a Keithley 230 programmable voltage source controlled by an HP 310 computer at various temperatures in the dark and under illumination by a solar simulator. Variation of J_{SC} vs V_{OC} was measured by varying the illumination intensity with neutral density filters for comparison with the dark current versus voltage variation. The capacitance versus voltage measurements were made using an HP 4275A LCR meter with a test signal of less than 20 mV, controlled by an HP 310 computer to measure the ionized impurity density and the depletion layer width in the dark and light. Absolute quantum efficiency measurements as a function of photon energy were also made.

III. EXPERIMENTAL RESULTS

A. Current versus voltage at room temperature

The forward-bias dark current density (J) versus voltage (V) characteristic of the ZnO/CdS/$CuInSe_2$ thin-film solar cell at room temperature is plotted in Fig. 2(a). The

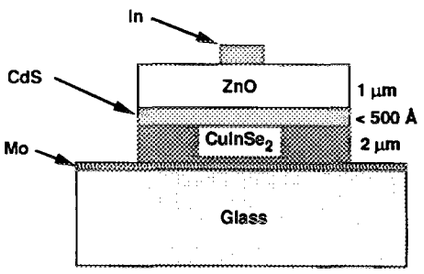

FIG. 1. Schematic diagram of the ARCO ZnO/CdS/$CuInSe_2$ solar cell.

[a] Present address: Electronics and Telecommunications Research Institute, P. O. Box 8, Daedog Danji, Daejon, Chungnam, Korea (South).

 0021-8979/90/214694-06$03.00

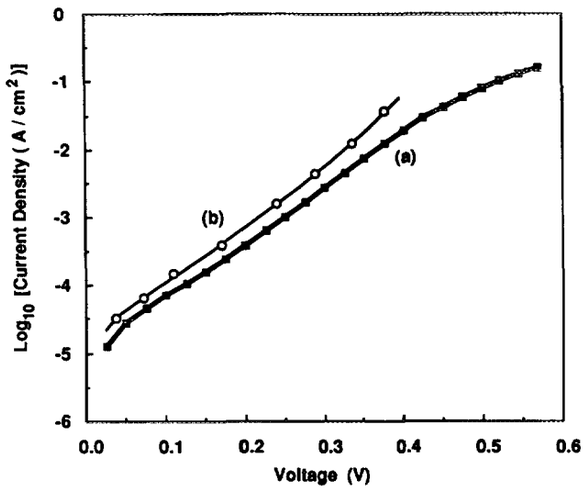

FIG. 2. Current density vs voltage for the ZnO/CdS/$CuInSe_2$ cell at 300 K, (a) J vs V in the dark, and (b) J_{SC} vs V_{OC}.

data were fit with a simulation program based on a standard single diode equation with series R_S and parallel R_p resistance correction:

$$J_f = (V - JR_S)/R_p + J_0 \exp\{[q(V - JR_S)/AkT] - 1\}, \quad (1)$$

where J_0 is the reverse saturation current and A is the diode factor. The value of R_S is determined independently from the inverse of the slope of a linear J-vs-V plot in the high forward bias region. The simulation yields $J_0 = 8.5 \times 10^{-6}$ A/cm^2 and $A = 1.9$ at room temperature. If these same values applied to the situation under illumination, an open-circuit voltage $V_{OC} = (AkT/q)\ln(J_{SC}/J_0) = 0.41$ V would be predicted.

Figure 3 compares the light and dark J-vs-V behavior of the cell. Under illumination with simulated sunlight of 100 mW/cm^2 intensity ($\sim$AM1.5), the cell shows $V_{OC} = 0.38$ V, $J_{SC} = 35.5$ mA/cm^2, and a fill factor (ff) of 0.61. Under large forward bias, the current density in the light exceeds the current density in the dark. If data under illumination conditions from Fig. 3 are plotted in the form of $\ln(J + J_{SC})$ vs V, where J is the total current under illumination, they can be approximately described by $J_{0l} = 3.3 \times 10^{-5}$ A/cm^2 and $A_l = 2.17$. The small decrease in V_{OC} measured under illumination, compared to the value predicted from the dark values of J_0 and A, arises primarily from a relatively small increase in J_0, partially compensated by a small increase in A. It is probable that there is no change in the transport mechanism as a result of illumination.

To provide further information about the junction transport in light, J_{SC} vs V_{OC} measurements were made and compared with the dark data, as shown in Fig. 2(b). The curve of J_{SC} vs V_{OC} does not show any hysteresis with the direction of changing light intensity. The difference between the dark J-V curve and the J_{SC}-V_{OC} curve in Fig. 2 is consistent with a small change in transport parameters with illumination.

B. Spectral response of quantum efficiency

Figure 4 shows the dependence of the quantum efficiency on wavelength without applied bias voltage. $CuInSe_2$, which has a direct band gap of about 1 eV, can generate a large photocurrent for wavelengths up to 1.3 μm. If the photocurrent is calculated based on the 100 mW/cm^2 ASTM AM1.5 global spectrum and assuming a completely transparent window layer, the maximum photocurrent is about 48–50 mA/cm^2, compared to the measured value for this cell of 35.5 mA/cm^2. A large portion of the loss of photocurrent is in the red response in the range above 0.9 μm, which may result from ZnO free carrier absorption and/or a small diffusion length of minority carrier electrons in $CuInSe_2$.

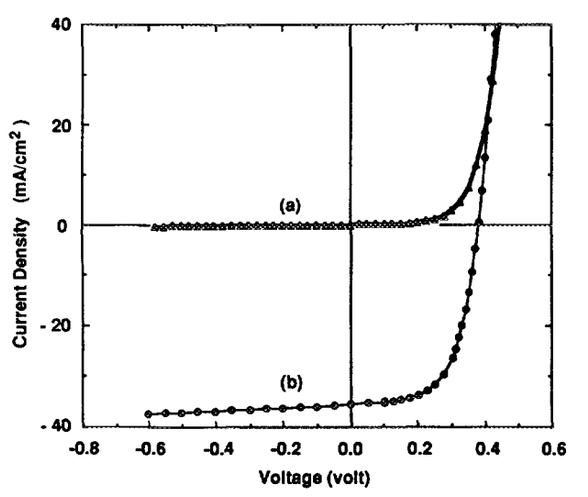

FIG. 3. Current density vs voltage for the ZnO/CdS/$CuInSe_2$ cell (a) in the dark and (b) under illumination with simulated sunlight of 100 mW/cm^2 intensity at 300 K.

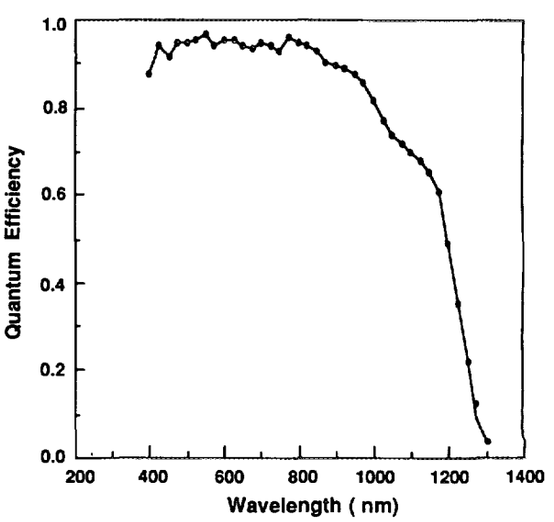

FIG. 4. Spectral dependence of the quantum efficiency of the ZnO/CdS/$CuInSe_2$ cell at 300 K without applied bias.

C. Capacitance measurements

To obtain further information on junction properties, the capacitance (C) of the cells was measured as a function of frequency and applied voltage. Most capacitance measurements were made at 100 kHz where the cells showed a minimum dissipation factor. To avoid the effect of parallel conductance, measurements were carried out in the parallel mode, where the measured impedance of the cell is assumed to be the result of a capacitor and resistor connected in parallel. The series resistance of the cell is about 0.4 Ω cm^2, which should not cause any problems.

Figure 5(a) shows the variation of capacitance with frequency. As the frequency increases, the capacitance decreases, indicating the existence of deep levels, which are commonly observed in other $CuInSe_2$-based solar cells.[11,15,16]

Figure 5(b) shows the dependence of $1/C^2$ on applied voltage. In a simple model, the extrapolation of $1/C^2$ to the voltage axis should give the diffusion potential, but in this case $1/C^2$ vs V is not a straight line and the extrapolation cannot be carried out meaningfully. Such a curved $1/C^2$-vs-V plot may result from a concentration gradient, deep levels in the $CuInSe_2$ or interface states at the CdS-$CuInSe_2$ interface.

Figure 5(c) shows the net negative charge in the $CuInSe_2$ depletion layer (since deep states are involved,[17] this is not the same as the free hole density) versus depletion width profile. At zero bias voltage the depletion width is 0.3–0.4 μm.

D. Dark current versus voltage measurements at various temperatures

Current versus voltage characteristics were measured at various temperatures in the dark between 210 and 360 K to provide further data on which to base modeling of the junction transport. Forward-bias J-vs-V curves were analyzed according to Eq. (1), and reverse-biased J-vs-V curves were analyzed according to Eq. (2):

$$J_r = (V - JR_S)/R_p + J_0\{\exp[q(V - JR_S/AkT)] - 1\}(1 - V)^{1/2}. \quad (2)$$

Here the square root in the second term on the right correlates the depletion region width with a chosen diffusion potential, $V_D = 1$ V.

Figure 6 shows the dark log J-vs-V characteristics of the cell at different temperatures. The values of R_S, R_p, J_0, and A required to fit the data are summarized in Table I.

Figure 7 shows the variation of the dark diode factor A and the voltage factor, $\alpha = 1/(AkT)$, as a function of tem-

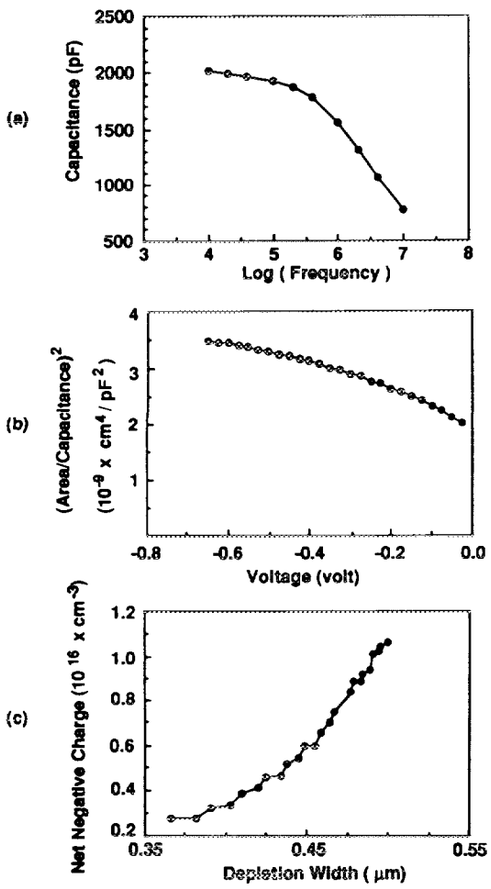

FIG. 5. Capacitance measurements for the ZnO/CdS/$CuInSe_2$ cell at 300 K. (a) Capacitance vs frequency, (b) (Area/capacitance)^2 vs applied voltage, and (c) net negative charge vs depletion width.

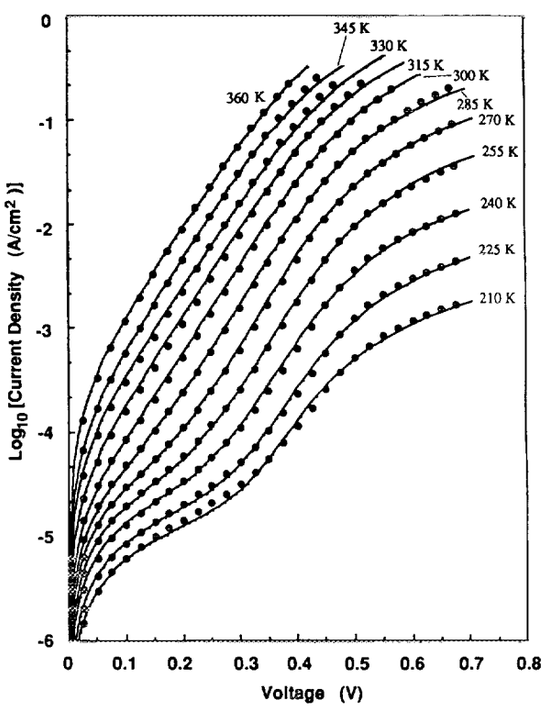

FIG. 6. Current density vs voltage in the dark for the ZnO/CdS/$CuInSe_2$ cell at temperatures ranging from 210 to 360 K. Data points are experimental; curves are results of simulation.

TABLE I. Dark diode parameters of a ZnO/CdS/$CuInSe_2$ cell. Values of R_S were obtained from the high bias slope of the linear J-V curve. A, J_0, and R_p were obtained by the curve-fitting program.

T (K)	A (V)	J_0 (A/cm^2)	R_p (10^3 Ω − cm^2)	R_S (Ω − cm^2)
210	2.1	4×10^{-9}	17	120
225	2.1	1.5×10^{-8}	12	40
240	2.07	6.8×10^{-8}	8	13
255	2.0	2.2×10^{-7}	6	4.0
270	1.9	6.5×10^{-7}	4.5	1.75
285	1.9	2.6×10^{-6}	4	0.85
300	1.9	8.5×10^{-6}	4	0.4
315	1.85	2.2×10^{-5}	3.5	0.3
330	1.85	5.2×10^{-5}	3.5	0.2
345	1.7	8.5×10^{-5}	3.5	0.2
360	1.7	2.0×10^{-4}	3.5	0.1

perature. The values of A, lying between 2.1 at 210 K and 1.7 at 360 K, suggest that recombination may be the dominant junction transport mechanism. At the same time, the variation of the voltage factor α with temperature suggests that thermally assisted tunneling could be an alternative mechanism for junction transport. Both of these mechanisms are discussed further later. It can be concluded at this point, however, that the observed variation of α with temperature rules out the model of multistep tunneling proposed by Riben and Feucht,[18] which requires a temperature independent α. Figure 8 shows that the J_0 for the cell has a temperature activation energy of 0.47 eV.

IV. DISCUSSION OF RESULTS

A. Transport mechanisms in the dark

Various transport models can be considered in view of the measured dependence of A and J_0 on temperature.

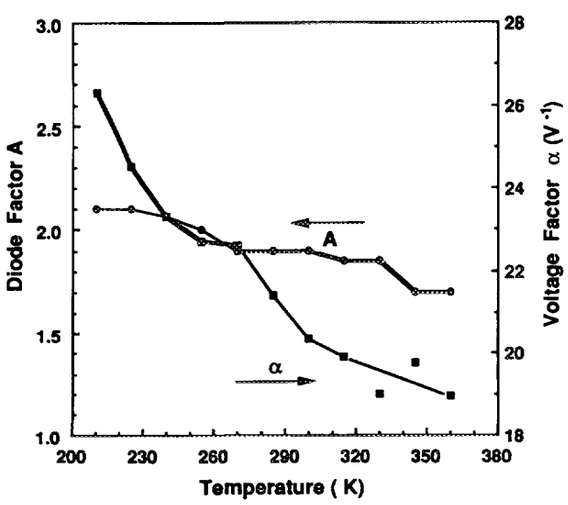

FIG. 7. Temperature dependence of the dark diode factor A and the dark voltage factor α for the ZnO/CdS/$CuInSe_2$ cell.

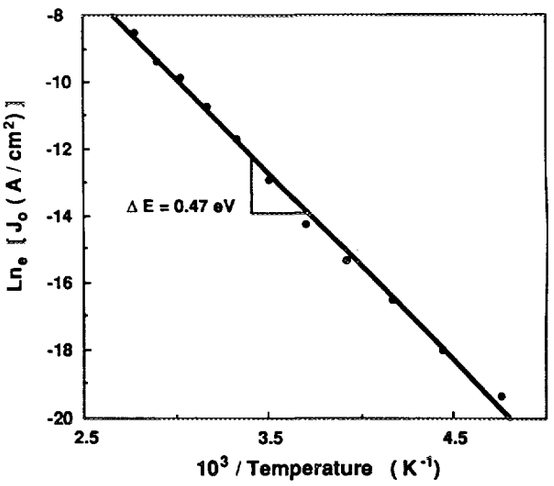

FIG. 8. Dark reverse saturation current J_0 as a function of inverse temperature for the ZnO/CdS/$CuInSe_2$ cell.

If interface recombination were a dominant transport mechanism, A should be approximately unity because the carrier density in the ZnO is much larger than that in the $CuInSe_2$. The activation energy of a ln J_0-vs-$1/T$ plot (recombination at interface is the limiting step) or a ln (J_0 T^{-2})-vs-$1/T$ plot (supply of holes to the interface is the limiting step) should be approximately equal to ($V_D + \partial_p$), where V_D is the diffusion potential of the cell and ∂_p is the energy difference between the Fermi level and the top of the valence band in the bulk $CuInSe_2$. The measured values of A lie between 1.7 and 2.1, much larger that the expected value of unity. The activation energies for a ln J_0-vs-$1/T$ plot and a ln ($J_0 T^{-1/2}$)-vs-$1/T$ plot are 0.47 and 0.43 eV, respectively, smaller than 1 eV, the calculated diffusion potential of the cell, assuming an electron affinity of 4.5 eV for $CuInSe_2$. We conclude that interface recombination is not the dominant mechanism of the ZnO/CdS/$CuInSe_2$ cell.

To test the suitability of a model based on recombination/generation in the depletion layer, a ln($J_0 T^{-2.5}$)-vs-$1/T$ plot was made as shown in Fig. 9. This model predicts that the activation energy of such a plot should be equal to approximately half the band gap. The activation energy found in Fig. 9 is 0.42 eV, close to half of the 1.0 eV band gap of $CuInSe_2$. In this recombination model, the value of A changes with properties of the recombination center, such as energy and capture cross section for electrons and holes, with the type of center (donorlike or acceptorlike), and with bias voltage.[19,20] The observed variation of A with temperature is small compared to what would be expected from the possible tunneling models discussed following. We conclude that recombination in the depletion region could be the dominant transport mechanism in the dark.

To test the possibility of tunneling currents in the cell, the data have also been considered in terms of the thermally assisted tunneling model proposed by Stratton and Padovani,[21] and the multistep tunneling model proposed by Riben and Feucht.[18] Figure 10 compares the change of the calculated α with temperature, based on these models with

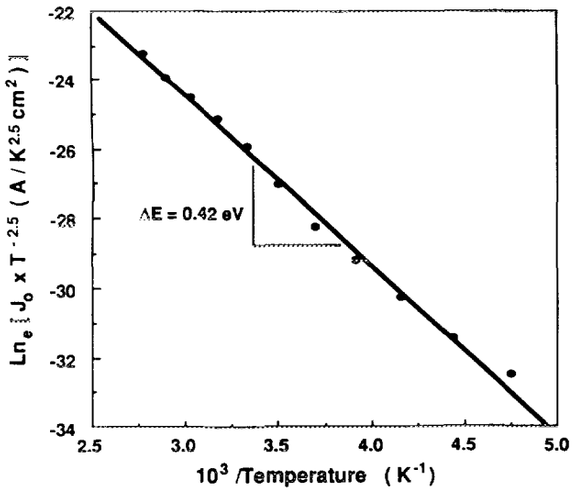

FIG. 9. A plot of $\ln (J_0 T^{-2.5})$ vs $1/T$ for the ZnO/CdS/$CuInSe_2$ cell in the dark.

the assumption of the rather high values of ionized acceptor density indicated in the figure caption, with the experimental data. The experimental data are most accurately described by the thermally assisted tunneling model. If thermally assisted tunneling were indeed the dominant mechanism, a plot of

$$\log [J_0 \cosh (E_{00}/kT) \coth (E_{00}/kT)^{1/2}] \text{ vs } \alpha$$

[where $E_{00} = (q\hbar/2)(N_A/\epsilon m^*)^{1/2}$ with N_a the density of ionized acceptors in the $CuInSe_2$, ϵ the dielectric constant, and m^* the hole effective mass] should be thermally activated with an energy of $(V_D + E_{fp})$ where E_{fp} is the height of the Fermi level above the valence edge in $CuInSe_2$. Such a plot shown in Fig. 11 has an activation energy of 1.5 eV, close to the calculated value of 1.2 eV, assuming a net charge density of 6×10^{18} cm.$^{-3}$ The fact that this effective ionized acceptor density in the tunneling region is much larger than the ionized acceptor density in the bulk does not appear, in itself, to be a conclusive argument against application of the thermally assisted tunneling model. Other research on ZnO/CdTe,[22] ZnO/InP,[23] and CdS/ZnCdTe junctions,[24] has shown similar effects.

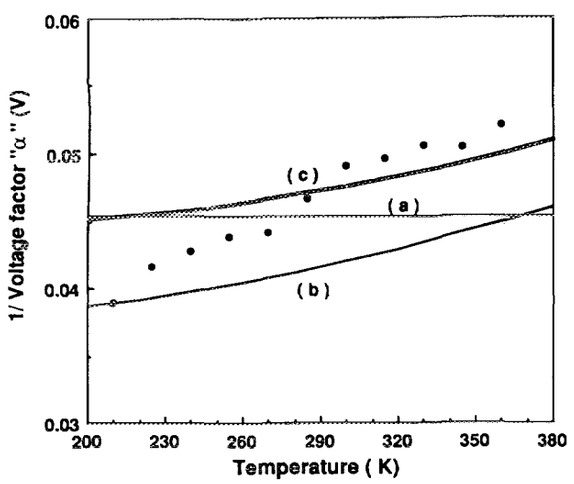

FIG. 10. Temperature dependence of $1/\alpha$ for the ZnO/CdS/$CuInSe_2$ cell in the dark compared to calculated curves corresponding to different tunneling models: (a) multistep tunneling, (b) thermally assisted tunneling with $N_A = 5\times10^{18}$ cm^{-3}, and (c) thermally assisted tunneling with $N_A = 7\times10^{18}$ cm^{-3}. An effective tunneling hole mass of 0.1 m_0 has been assumed.

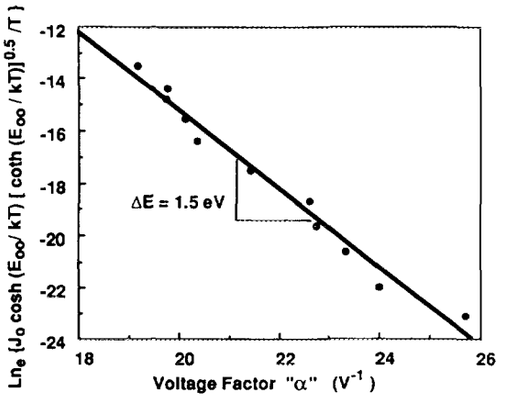

FIG. 11. Variation of dark J_0 vs α, corresponding to a thermally assisted tunneling model for the ZnO/CdS/$CuInSe_2$ cell.

It must be concluded, therefore, that an analysis of the J-V characteristics in the dark, over the limited temperature range possible, does not allow us to distinguish unambiguously between junction transport dominated by recombination in the depletion layer, or thermally assisted tunneling.

V. SUMMARY

The ARCO ZnO/CdS/$CuInSe_2$ solar cells that we investigated show $V_{OC} = 0.36 - 0.42$ V, $J_{SC} = 35 - 40$ mA/cm^2, ff $= 0.5 - 0.65$, and cell efficiency $\eta = 7$–9% under illumination by simulated sunlight of 100 mW/cm^2 intensity.

Capacitance measurements indicate that deep levels are present in the $CuInSe_2$.

An analysis of J-V characteristics in the dark as a function of temperature shows that junction transport could be controlled either by recombination in the depletion region ($A \sim 1.9$, and $\ln J_0$-vs-$1/T$ activation energy of 0.42 eV, about half the band gap of $CuInSe_2$) or by thermally assisted tunneling (predicted temperature dependence of α if $N_A = 6\times10^{18}$ cm^{-3}, and $\ln J_0$-vs-α slope of 1.5 eV, close to the calculated value of 1.2 eV).

An analysis of J_{SC} vs V_{OC} indicates that the dominant junction-transport mechanism is affected by illumination. Analysis for J_{0l} and A_l values under illumination at room temperature indicates that both are slightly increased by illumination, yielding a slightly lower value of measured V_{OC} compared to values expected from the dark parameters.

ACKNOWLEDGMENTS

This research was supported by ARCO Solar (now Siemens Solar) Inc. The authors are grateful for this support and for the samples used in this research supplied by Dr. K. Mitchell and Dr. R. Potter.

[1]S. Wagner, J. L. Shay, P. Migliorato, and H. M. Kasper, Appl. Phys. Lett. **25**, 434 (1974).
[2]L. L. Kazmerski, in *Ternary Compounds* 1977, edited by G. D. Holah, (Institute of Physics, London, 1977), pp. 217–228.
[3]R. A. Mickelsen and W. S. Chen, in *Proceedings of the 16th IEEE Photovoltaic Specialists Conference*, 781 (IEEE, New York, 1982).
[4]W. E. Devaney, R. A. Mickelsen, S. Chen, J. M. Stewart, Y. R. Hsiao, L. C. Olsen, and A. Rothwarf, Boeing First Quarter SERI Technical Report, (1985) p. 8.
[5]R. R. Potter, C. Eberspacher, and L. B. Fabick, in *Proceedings of the 17th IEEE Photovoltaic Specialists Conference*, 1659 (IEEE, New York, 1985).
[6]W. A. Miller and L. C. Olsen, IEEE Trans. Electron Devices **ED-31**, 654(1984).
[7]R. R. Potter and J. R. Sites, IEEE Trans. Electron Devices **ED-31**, 571 (1984).
[8]A. Rothwarf, IEEE Trans. Electron Devices **ED-31**, 1513 (1982).
[9]N. M. Eron and A. Rothwarf, in *Proceedings of the 17th Photovoltaic Specialists Conference*, 876 (IEEE, New York, 1984).
[10]R. R. Potter, Solar Cells **16**, 521 (1986).
[11]R. K. Ahrenkiel, Solar Cells **16**, 549 (1986).
[12]A. Rothwarf, Solar Cells, **16**, 567 (1986).
[13]S. Damasknos, J. D. Meakin, and J. E. Phillips, in *Proceedings of the 19th IEEE Photovoltaic Specialists Conference*, 1299 (IEEE, New York, 1987).
[14]K. Mitchell and H. I. Liu, in *Proceedings of the 20th IEEE Photovoltaic Specialists Conference*, 1461 (IEEE, New York, 1988).
[15]R. Haak, S. Menezes, and K. J.. Bachmann, in *Proceedings of the 19th IEEE Photovoltaic Specialists Conference*, 961 (IEEE, New York, 1987).
[16]V. Ramanathan, R. Noufi, and R. C. Powell, J. Appl. Phys. **63**, 1203 (1988).
[17]J. J. Shiau, A. L. Fahrenbruch, and R. H. Bube, J. Appl. Phys. **59**, 2879 (1986).
[18]A. R. Riben and D. L. Feucht, Int. J. Electron. **20**, 583 (1966).
[19]C. T. Sah, R. N. Noyce,and W. Shockley, Proc. IRE **45**, 1228 (1957).
[20]S. C. Choo, Solid-State Electron. **11**, 1069 (1968).
[21]F. A. Padovani and R. Stratton, Solid-State Electron. **9**, 695 (1966).
[22]J. A. Aranovich, D. Golmayo, A. L. Fahrenbruch, and R. H. Bube, J. Appl. Phys. **51**, 4260 (1980).
[23]C. Eberspacher, A. L. Fahrenbruch, and R.H. Bube in *Proceedings of the 17th IEEE Photovoltaic Specialists Conference*, 459 (IEEE, New York, 1984).
[24]M. G. Peters, A. L. Fahrenbruch, and R. H. Bube, J. Appl. Phys. **64**, 3106 (1988).